Influence of pH on mechanical relaxations in high solids LM-pectin preparations

ARTICLE *in* CARBOHYDRATE POLYMERS · AUGUST 2015

Impact Factor: 4.07 · DOI: 10.1016/j.carbpol.2015.03.051

3 AUTHORS, INCLUDING:

Katerina Alba

University of Huddersfield

4 PUBLICATIONS **15** CITATIONS

SEE PROFILE

Vassilis Kontogiorgos

University of Huddersfield

34 PUBLICATIONS **368** CITATIONS

SEE PROFILE

Carbohydrate Polymers 127 (2015) 182–188

Contents lists available at ScienceDirect

Carbohydrate Polymers

journal homepage: www.elsevier.com/locate/carbpol

Influence of pH on mechanical relaxations in high solids LM-pectin preparations

K. Alba [a], S. Kasapis [b], V. Kontogiorgos [a,*]

[a] Department of Biological Sciences, University of Huddersfield, Huddersfield HD1 3DH, UK
[b] School of Applied Sciences, RMIT University, City Campus, Melbourne 3001, VIC, Australia

ARTICLE INFO

Article history:
Received 18 January 2015
Received in revised form 12 March 2015
Accepted 13 March 2015
Available online 30 March 2015

Keywords:
Pectin
Okra
Relaxation
Glass transition
DSC

ABSTRACT

The influence of pH on the mechanical relaxation of LM-pectin in the presence of co-solute has been investigated by means of differential scanning calorimetry, ζ-potential measurements and small deformation dynamic oscillation in shear. pH was found to affect the conformational properties of the polyelectrolyte altering its structural behavior. Cooling scans in the vicinity of the glass transition region revealed a remarkable change in the viscoelastic functions as the polyelectrolyte rearranges from extended (neutral pH) to compact conformations (acidic pH). This conformational rearrangement was experimentally observed to result in early vitrification at neutral pH values where dissociation of galacturonic acid residues takes place. Time–temperature superposition of the mechanical shift factors and theoretical modeling utilizing WLF kinetics confirmed the accelerated kinetics of glass transition in the extended pectin conformation at neutral pH. Determination of the relaxation spectra of the samples using spectral analysis of the master curves revealed that the relaxation of macromolecules occurs within ~0.1 s regardless of the solvent pH.

1. Introduction

Relaxation studies are frequently employed in biopolymer systems as a probe to shed light on macromolecular rearrangements. These motions in turn are pertinent to vitrification that is responsible for the mechanical performance and stability of biopolymer glasses. In the low moisture (or high solids) regime, including those found in dehydrated or frozen foods and low moisture pharmaceutical formulations (*e.g.*, tablets, powders), biopolymers are of particular importance in both academic and industrial fields. To that end, mechanical and thermal relaxations are commonly employed in the study of viscoelasticity for natural polymers and are now well understood so as to draw structure–function relationships (Kasapis, 2012).

Pectic polysaccharides traditionally play a central role as major components in the development of high-solid confectionery products (Al-Ruqaie, Kasapis, Richardson, & Mitchell, 1997; Almrhag et al., 2012; Kasapis, Al-Alawi, Guizani, Khan, & Mitchell, 2000a). Recently, their ability to create systems for controlled delivery of bioactives was also explored (Panyoyai, Bannikova, Small, & Kasapis, 2015). In previous investigations, high methoxylated (HM) pectin from citrus sources was utilized to explore the relaxation properties of the pectin–co-solute systems. The structural simplicity and usually low molecular weight of HM-pectin allows gelation under high solid (>~50%) and low pH conditions (Evageliou, Richardson, & Morris, 2000). Depending on the chemical nature of the sugar employed (monosaccharide *vs.* disaccharide *vs.* polydisperse glucose syrups) the morphology of networks and their viscoelasticity may change dramatically (Kasapis, Al-Marhoobi, Deszczynski, Mitchell, & Abeysekera, 2003a).

To build on previous findings, we increase the structural complexity of the polysaccharide as the fine structure of pectin influences to a great extend its physical behavior (Kim et al., 2013; Strom et al., 2007) and we introduced pectin extracted from okra pods with distinct physicochemical behavior. The major structural elements of pectin include homogalacturonan segments that are mainly composed of α-D-galacturonic acid residues and rhamnogalacturonan-I (RG-I) regions consisting of repeating units of α-D-galacturonic acid and α-L-rhamnose monomers with arabinan and/or galactan side chains (Vincken et al., 2003). In contrast, pectin extracted from okra is distinct as it mostly contains RG-I units and is highly acetylated with low degree of methoxyl substitution (LM-pectin) (Alba, Laws, & Kontogiorgos, 2015; Sengkhamparn et al., 2009a; Sengkhamparn, Verhoef, Schols, Sajjaanantakul, & Voragen, 2009b).

We have previously demonstrated that glassy pectin-matrix tablets slow the kinetics of drug release and furthermore create

* Corresponding author. Tel.: +44 1484 472488.
E-mail address: v.kontogiorgos@hud.ac.uk (V. Kontogiorgos).

http://dx.doi.org/10.1016/j.carbpol.2015.03.051
0144-8617/

stable emulsions indicating that they could be exploited in drug or nutrient encapsulation and delivery (Alba, Ritzoulis, Georgiadis, & Kontogiorgos, 2013; Ghori, Alba, Smith, Conway, & Kontogiorgos, 2014). In the present work, we aim to gather further evidence on the influence of macromolecular conformations on the mechanical properties of pectin, as impacted by the degree of ionization in the presence of small molecular weight co-solutes.

2. Materials and methods

2.1. Pectin extraction

Isolation and characterization of pectin samples were carried out according to earlier published protocols. Briefly, okra pods were subjected to an aqueous extraction at pH 6.0, precipitated with ethanol, dialyzed and freeze-dried to obtain dry pectin isolate. Total sugar analysis, protein content and D-GalA content, degree of methylation and acetylation, molecular weight and intrinsic viscosity were all determined, as described in our previous work (Alba et al., 2015). The major physical and chemical characteristics that are relevant to this work are reproduced in Table 1.

2.2. Glucose syrup

Glucose syrup Sipa-Wheat 69 (Sipal Partners, Herve, Belgium) with 80% total solids and dextrose equivalent of 69 was used for sample preparation. The total carbohydrates on dry matter were 97.5% w/w and carbohydrates with degree of polymerization greater than 2 constituted 13.5% w/w of the syrup. Glucose and maltose were 35 and 49% w/w, respectively.

2.3. Sample preparation

Pectin dispersions were prepared by dissolving the isolated polysaccharide at 1% (w/w) in either citric (pH 3.0) or phosphate (pH 7.0) buffers (100 mM) at room temperature under continuous stirring. Following dispersion of the polysaccharide, the temperature was raised to 70 °C and the appropriate amount of glucose syrup was added. The mixture was maintained at 70 °C until the required total solids content was obtained (80% w/w) by slowly evaporating water.

2.4. Rheological measurements

These were performed using a Bohlin Gemini 200HR-nano rotational rheometer (Malvern Instruments, Malvern, UK) equipped with plate-plate geometry (20 mm diameter and 1 mm gap). Temperature was controlled with a Peltier supported by a low temperature ethylene glycol bath (Julabo, F12, Germany) able to reach −30 °C. Experimental protocol of the present investigation included the following steps: Cooling scans were performed between 20 and −30 °C at a cooling rate of 2 °C/min, 0.01% strain and angular frequency of 1 rad/s. To investigate the viscoelastic behavior of the systems and create master curves of viscoelasticity, frequency sweeps were performed within the range of 0.628–62.8 rad/s at a strain of 0.01% with 4.4 °C temperature intervals. Modeling of rheological data was performed on Prism v.6 (Graphpad Software, San Diego, USA).

Table 1
Chemical and physicochemical properties of okra pectin isolate.

D-GalA[a]	56.9 ± 6.9
Degree of methylation (DM%)	24.6 ± 1.0
Degree of acetylation (DA%)	37.6 ± 3.0
Total sugars[a]	81.8 ± 6.4
Protein[a]	6.3 ± 0.1
$M_w \times 10^3$ (g/mol)	767
$[\eta]$ (dL/g)	4.4 (at pH 7.0) or 2.8 (at pH 3.0)

[a] All values are expressed as % on wet basis of the pectin powder.

2.5. Differential scanning calorimetry

Thermal analysis was performed using a Star System DSC1 (Mettler Toledo, Switzerland) with a Huber TC100 cooling system (Huber, Germany) to achieve temperatures down to −90 °C and a nitrogen DSC-cell purge at a flow rate of 50 ml/min. Samples with total solids of 80% (w/w) were weighed (about 15 mg) and hermetically sealed in aluminum pans, which were cooled from 10 to −90 °C at 2 °C/min. First derivative curve of heat flow and estimation of glass transition temperatures were determined with STARe Evaluations software supporting the instrument (v. 12.1, Mettler Toledo, Switzerland).

2.6. ζ-Potential titration

These measurements were performed using a ZetaSizer Nano Series ZEN2600 (Malvern Instruments, Malvern, UK) at 25 °C. Pectin solutions were dispersed at 0.625% w/v in citric buffer (100 mM) at pH 3.0 and titration was performed with 0.75 M sodium hydroxide to pH 7.0 or 0.75 M hydrochloric acid to pH 1.0. All measurements were performed in duplicates.

2.7. Numerical computation

This was performed in MATLAB (v7.0 R14 Service Pack 2, The Mathworks Inc., MA). The first step involves discretization of the viscoelastic functions of G' or G'' to create matrix A and was performed with the *discrG.m* script published elsewhere (Kontogiorgos, 2010). Following that step, algorithms *csvd.m* for calculation of the singular value decomposition of the matrix A and *l_curve.m* for computation of the optimum regularization parameter were used from Hansen's regularization tools package (Hansen, 1994). Finally, the algorithm *NLCSmoothReg.m* was used for the calculation of the relaxation spectra (Wendlandt, 2005).

3. Results and discussion

3.1. Sample characterization and viscoelasticity of pectin–co-solute mixtures

The pectin isolate used in the present investigation is of high purity (low protein concentration and high total carbohydrates) and high molecular weight (Table 1). Intrinsic viscosities were determined at two different pH values (7.0 and 3.0) matching those in sample preparation. These measurements were performed under the electrostatic screening of 0.1 M NaCl. This approach masks non-specific electrostatic interactions so that changes in coil dimensions are attributed to changes in the degree of ionization with variation of buffer pH (citric and phosphate). It is evident that pH plays a decisive role in coil dimensions resulting in an expanded conformation due to dissociation of D-GalA at high pH values (Table 1). It is expected that the high co-solute concentration (glucose syrup) in the samples will have an influence on the conformational properties of pectin as solvent quality changes. It has been reported for β-glucan (Grimm, Kruger, & Burchard, 1995), guar and locust bean gum (Richardson, Willmer, & Foster, 1998) and seed gums (Behrouzian, Razavi, & Karazhiyan, 2014; Mohammad Amini & Razavi, 2012) that intrinsic viscosity reaches a minimum before starting increasing again depending on the sugar type and concentration.

This has been attributed to changes in the solvent quality as sugar concentration varies up to 40% w/w solids, and to the degree

or extent of inter- and intra-chain interactions (Richardson et al., 1998). Clearly, intrinsic viscosity measurements are difficult to perform at higher levels of solids, but we are aware that at the level of solids in this investigation (80% w/w) competition for water changes the phase morphology of our preparation paving the way for molecular phenomena of glassy consistency with decreasing temperature. Quoted values of intrinsic viscosity in Table 1 serve the purpose of demonstrating the effect of pH (from 7.0 to 3.0) on the conformational characteristics of the polymer. Thus, hydrodynamic volume can be modulated by changes in the degree of ionization, and this modification of macromolecular interactions controls the viscoelasticity of the samples, which is the subject of focus in this investigation.

Determination of functional groups content revealed that the polyelectrolyte is a low methoxylated pectin (LM) with a high degree of acetylation (DA) and an intermediate D-GalA content (Table 1). Branching analysis of the sample showed high contribution of RG-I units (~60%) to the pectin backbone whereas the remaining units were HG segments indicating a highly branched biopolymer (Alba et al., 2015). At this juncture, it should be mentioned that preparation of polysaccharide solutions at alkaline or acidic pH might affect their structural characteristics. In general, polysaccharides may undergo degradation reactions in relation to the pH of the system. For instance, β-elimination and peeling degradation reactions occur at elevated pH values whereas acid hydrolysis upon prolonged exposure to low pH values. However, reduced water content and mobility due to the presence of high levels of glucose syrup (79% w/w) dramatically decelerate hydrolysis in our materials, since water is largely unavailable to participate in chemical reactions. Furthermore, the resistance of D-GalA glycosidic bond to both acidic and alkaline hydrolysis (due to inductive effects of the carboxyl group at C-5) and the limited time that the sample remains at elevated temperatures during sample preparation (~15 min) minimize potential hydrolytic reactions. Therefore, prominent molecular characteristics from the original material remain and allow meaningful comparisons in this investigation regarding the effect of degree of ionization (pH variation from 3.0 to 7.0) on vitrification phenomena.

Gelation in low methoxylated pectin is mediated by electrostatic bridging of adjacent carboxyl groups of D-GalA residues typically with calcium cations or in some instances with monovalent ions (Strom, Schuster, & Goh, 2014). Sol–gel transition, however, is frequently interrupted by the presence of side chains or acetyl groups that moderate the ability of the polymer to gel. Okra pectin is distinct because it primarily consists of RG-I units and has a high acetyl content virtually halting the gelation process. Preliminary work on our pectin in the absence of glucose syrup confirmed that it remained in the sol state under an extensive set of experimental conditions (*e.g.*, calcium and pectin concentration, pH, temperature).

The following discussion deals with molecular relaxations of LM pectin–co-solute mixtures at total solids of 80% (w/w) and acidic or neutral pH (3.0 or 7.0) in the absence of network formation. Calorimetric measurements provide a first insight into the macromolecular relaxations. Usually, polydisperse polymers vitrify over a broad range of temperatures as the intermolecular energy barriers to segmental and group motions exhibit a broad distribution (Bohmer, Ngai, Angell, & Plazek, 1993; Roland, 2010). Fig. 1 shows calorimetric traces of glucose syrup and high-solid mixtures at two different pH values. The onset of glass transition temperature was estimated by the crossover of the tangents of first derivative curve of heat flow at the onset of the transition (Fig. 1, bottom right inset). The midpoint of glass transition temperature was estimated at the midpoint between the tangents of the heat flow curve before and after the transition (Fig. 1).

The onset and mid-point glass transition temperatures for glucose syrup were estimated to be at −35 and −53 °C, respectively. The pectin–glucose syrup mixtures at pH 3.0 revealed only marginal differences from its counterpart in the absence of pectin, with the onset and midpoints being −31 and −48 °C, respectively. However, switching pH to 7.0 accelerates vitrification events for pectin–glucose syrup samples to more than eight degrees (−27 °C (onset) and −45 °C (midpoint)). The first derivative of a glass transition gives a peak whose area is proportional to the value of Δc_p (Fig. 1, bottom right inset). Peak temperatures of the first derivative can be used as a measure of changes in T_g or for the comparison of the effects of different treatments (Haines, Reading, & Wilburn, 2003). Analysis of calorimetric traces in Fig. 1 with this approach showed peak maxima at −55, −56 and −49 °C for glucose and high solids pectin samples at pH 3 and 7, respectively. Treatment of

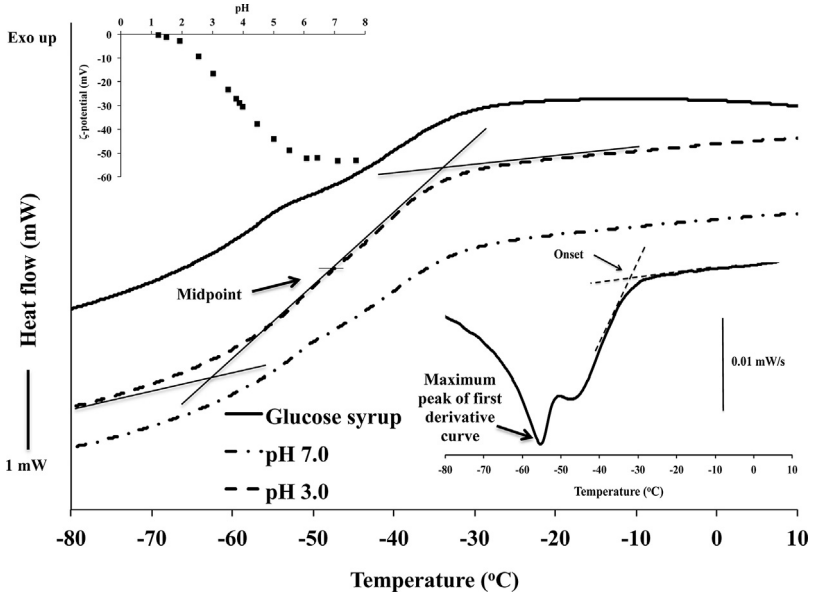

Fig. 1. DSC thermograms of 80% glucose syrup and 1% LM-pectin plus 79% glucose syrup at pH 3.0 and 7.0. Top left inset shows ζ-potential titration of the pectin solution. Bottom right inset shows a typical first derivative curve of heat flow of the samples and calculations used to derive the onset of the glass transition.

calorimetric data revealed the pH-induced influence of the polyelectrolyte conformation on calorimetric relaxation of the samples. Such a behavior calls for further exploration on the effect of pH on macromolecular conformation of our samples.

Top left inset in Fig. 1 shows results on the ζ-potential titration of the pectin. It is evident that from pH 6.0 upwards, D-GalA residues on the polymeric backbone are fully dissociated. This yields an extended conformation in the macromolecule, an outcome that is also reflected in the intrinsic viscosity values of the sample discussed in Table 1. On the other hand, the compact molecular arrangement at pH 3.0 creates strong intra-chain associations as the charge is neutralized at around pH 1.0. A compact polymeric structure increases the overall free volume of the pectin–glucose syrup mixture as the hydration and interaction of the polyelectrolyte with water and co-solute is restricted. This enhances the dominance of the co-solute in mixture with pectin at pH 3.0 leading to a vitrification pattern that is similar to the single glucose-syrup preparation in the DSC thermograms (Fig. 1).

The influence of pH on pectin conformation should also play a central role in the mechanical properties of the high-solid samples. It is possible to monitor mechanical developments on cooling of our samples by employing well-established approaches from the synthetic polymer science. The dependence of storage and loss modulus on temperature at pH 3.0 and 7.0 close to the onset of the calorimetric glass transition regime is recorded down to −28 °C in Fig. 2. In both cases, G'' is higher than G' throughout the experimental temperature range, a behavior that is typical of viscous materials. Clearly, viscoelastic functions at pH 7.0 are two orders of magnitude greater than the low pH counterparts. This is a direct evidence of the role of intermolecular interactions in the mechanical properties, with the extended pectin conformation at pH 7.0 increasing the elastic character of the mixture.

An approach to extend monitoring the viscoelastic parameters beyond the experimentally accessible range is to utilize the time–temperature superposition principle. When materials do not exhibit structural transitions (*e.g.*, gelation, melting or denaturation) during the course of measurement, the viscoelastic modulus measured at a set of frequencies and temperatures (ω, T) is equivalent to measurements taken at frequency ω multiplied with a shift factor (a_T) (Mezger, 2011). The master curve at a convenient

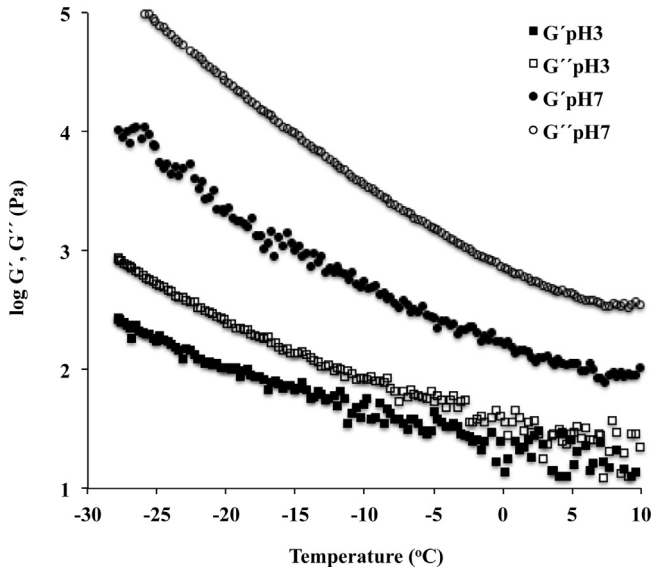

Fig. 2. Temperature dependence of the storage and loss modulus for systems containing 1% LM-pectin and 79% glucose syrup at pH 3.0 and 7.0 (scan rate: 2 °C/min; frequency: 1 rad/s; strain: 0.01%).

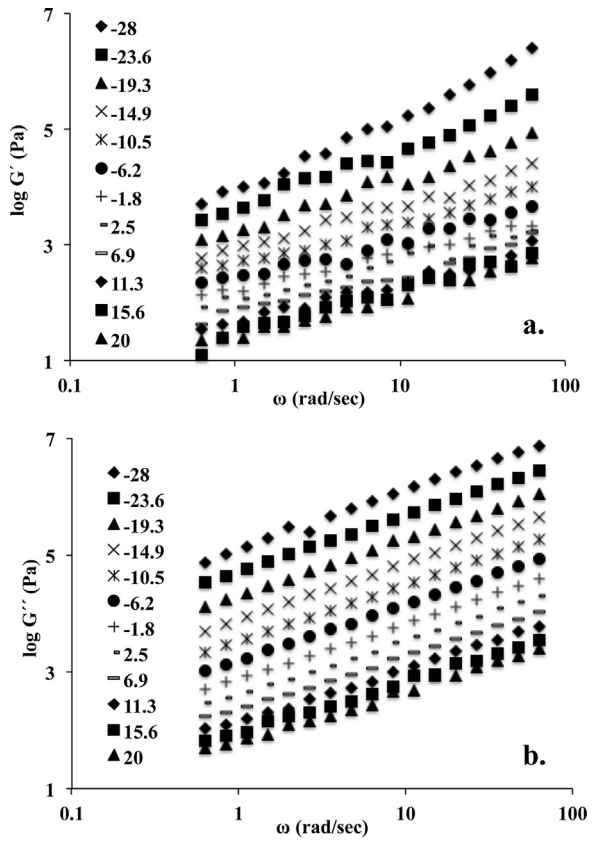

Fig. 3. Double logarithmic plots of (a) storage and (b) loss modulus against frequency of oscillation for a sample containing 1% LM-pectin and 79% glucose syrup at pH 7.0 (temperature interval: 4.4 °C; strain: 0.01%).

reference temperature T_o can then be obtained by plotting the viscoelastic functions *vs.* ωa_T. In doing so, frequency sweeps were carried out at temperature intervals of 4.4 °C from 20 to −28 °C in Fig. 3. Enhanced intermolecular associations are evident with lowering temperature as the storage and loss modulus values are becoming progressively higher. Plateauing of the values, however, is not observed, which is typical of polymers well within the glassy state. In order to calculate the horizontal shift factors, we used the method of reduced variables ($a_T = \omega_r/\omega$) at the reference temperature of $T_o = -19$ °C. The reference temperature is usually chosen to be near to the operating temperature of the biopolymer. In our case, we have chosen a temperature that is well within the glass transition range of our biopolymer in order to appreciate the influence of pH in macromolecular dynamics.

Fig. 4 illustrates the results of the aforementioned treatment for the mechanical spectra in Fig. 3. The master curves of viscoelasticity extend over four orders of magnitude in frequency revealing relaxation patterns that correspond to the glass transition region of the sample at pH 7.0. To further explore the effect of temperature, horizontal shift factors, a_T, were plotted against $T–T_o$ in Fig. 5. This approach provides information about the temperature dependence of molecular mobility upon which the various relaxation mechanisms depend (Williams, Landel, & Ferry, 1955). It appears that below about 0 °C (or $T–T_o = 20$ °C) shift factors exhibit a strong temperature dependence indicating a transition to distinct relaxation kinetics with reduced temperature. This commonly occurs as the sample enters the glass transition region in high-solid biopolymer systems (Al-Ruqaie et al., 1997; Jiang, Kasapis, & Kontogiorgos, 2011; Kasapis, Al-Marhoobi, & Khan, 2000b). Free volume theory

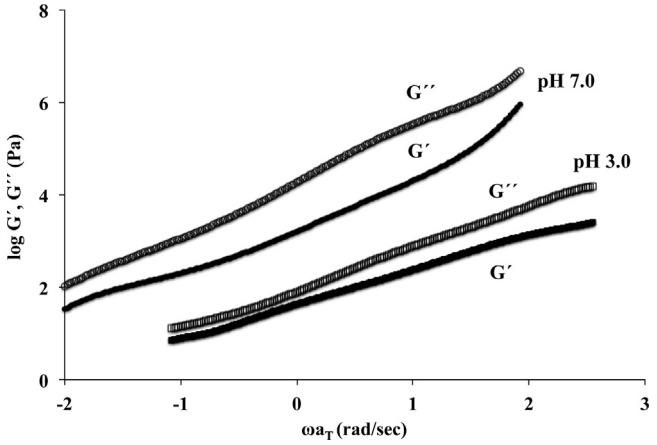

Fig. 4. Master curves of viscoelasticity as a function of reduced frequency of oscillation (ωa_T) for systems containing 1% LM-pectin and 79% glucose syrup at pH 3.0 and 7.0 at the reference temperature of −19 °C.

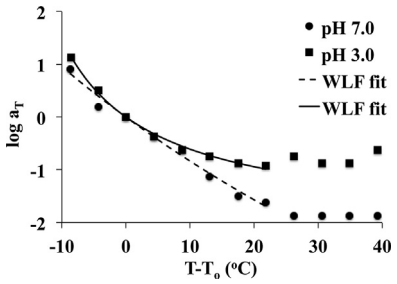

Fig. 5. Logarithmic shift factor, a_T, for systems containing 1% LM-pectin and 79% glucose syrup at pH 3.0 and 7.0 plotted against temperature from the data of the master curves presented in Fig. 4 (WLF fits are also shown for both samples).

and the empirical WLF equation are then employed to follow the process of vitrification:

$$\log\ a_T = \frac{C_1^o (T - T_o)}{C_2^o (T - T_o)} \quad (1)$$

C_1^o and C_2^o are the WLF constants at the reference temperature T_o and are related to the free volume theory as follows:

$$C_0^1 = \frac{B}{2.303 f_0}, C_0^2 = \frac{f_o}{\alpha_f} \quad (2)$$

where f_o is the fractional free volume at T_o, α_f is the thermal expansion coefficient and B is a constant that equals unity.

Utilization of this approach allows association of the concept of glass transition with fundamental quantities such as the evolution of free volume during vitrification. Our experimental setup captures a significant part of this event to return estimates of C_1^o, C_2^o, f_o and α_f at T_o in Table 2. Values of f_o for the sample at pH 7 is in good agreement with previously studied high-solid biopolymer mixtures (Al-Ruqaie et al., 1997) and amorphous synthetic polymers (Ferry, 1980) to demarcate the mechanical rubber-to-glass transition. In contrast, adjusting pH to 3 brings about a mechanical behavior with values of f_o being an order of magnitude higher than for the neutral pH counterpart. This behavior indicates that for these samples the glass transition region occurs at lower temperatures and could not be accessed in the temperature range we employed in the present work.

Table 2
Values of WLF Parameters for 1% LM-pectin and 79% glucose syrup at pH 3.0 and 7.0.

Sample	C_1^o	C_2^o (°C)	f_o	α_f ($\times 10^{-4}$ °C^{-1})
pH 3	2.07	24.12	0.209	86
pH 7	13.27	149	0.032	2.1

The above predictions are congruent with the cooling scans in Fig. 2 and the calorimetric data in Fig. 1 arguing that the high pH samples move toward the glassy state at a rapid rate. Electrokinetic potential measurements also in Fig. 1 indicate that D-GalA residues are fully dissociated at pH 7 resulting in electrostatic repulsion and an extended chain conformation. The macromolecular outcome is an efficient polymer hydration and interaction with glucose syrup that reduces the overall free volume in the mixture. Conversely, the compact pectin conformation at pH 3, due to the protonation of the D-GalA residues, results in a co-solute dominated matrix of increased diffusional mobility and free volume that delays vitrification.

Previous work on other gelling polysaccharide systems showed that the rheologically determined T_g is affected by the structural morphology, network strength and molecular weight of the biopolymer (Kasapis, 2008). Generally, the ability of the polysaccharide to form a network in the presence of high levels of co-solute accelerates vitrification events due to restricted diffusional mobility of the chains as, for example, it has been shown for κ-carrageenan with added potassium counterions (Evageliou, Kasapis, & Hember, 1998), high methoxy pectin (Almrhag et al., 2012), deacylated gellan with added sodium counterions (Al-Ruqaie et al., 1997) or gelatin of various molecular weights (Kasapis, Al-Marhoobi, & Mitchell, 2003b).

Present work highlights the importance of biopolymer conformation on the vitrification of high-solid polysaccharide systems. For instance, in gelling systems including κ-carrageenan and deacylated gellan, network formation is a kinetic process being influenced by the degree of ionization. This ultimately affects gel microstructure and how rapidly the system arrives at the onset of glass transition. Careful tuning of pH seems to be a prerequisite for this, but it somehow has escaped attention thus far. Conversely, the addition of small amounts of non-gelling polysaccharides such as guar or locust bean gum has little effect on the mechanical manifestation of vitrification (Kasapis et al., 2000b). The inability to form a network results in molecular mobility in the sugar matrix thus requiring lower temperatures to achieve the glassy state, and galactomannans show comparable glass transition regimes and fractional free volume values with non-gelling high methoxy pectin samples at pH 7.0. This behavior is distinct from observations on gelling citrus pectin in the presence of high levels of co-solute where the industrially relevant pH of 3.5 was used (Kasapis et al., 2000a). It should be noted that in neutral polysaccharides, pH effects on chain conformation are reduced, as solvent ionization does not exert the same influence as in polyelectrolytes. On the contrary, we demonstrated that in polyelectrolytes by drastically shifting the pH toward the p*K*a point changes in coil conformation result in remarkable modification in the mechanical properties of the system.

Findings of the present work extend to other low-moisture glassy systems incorporating non-gelling polysaccharides for various industrial applications. For instance, encapsulation methods (spray drying and electrospraying) or edible film formation utilizes a wide range of carbohydrate polymers and co-solutes to formulate matrices of glassy consistency (Espitia, Du, Avena-Bustillos, Soares, & McHugh, 2014; Fathi, Martin, & McClements, 2014). Understanding the underlying molecular mechanism of polyelectrolyte vitrification and the structural relaxations occurring in glass transitions assists in controlling optimum fabrication in industrially relevant preparations.

3.2. Calculation of relaxation spectra

It is possible to determine the time needed for the completion of macromolecular motion with the help of a relaxation spectrum. Appropriate conversion of mechanical spectra from master curves can be used to calculate the relaxation spectra of biopolymers. The relationship between the storage modulus, loss modulus and angular frequency (ω) in shear is given by the following integrals (Tschoegl, 1989):

$$G'(\omega) = G_o + \int_0^\infty H(\tau)\frac{\omega^2\tau^2}{1+\omega^2\tau^2}\frac{d\tau}{\tau} \quad (3)$$

$$G''(\omega) = \int_0^\infty H(\tau)\frac{\omega\tau}{1+\omega^2\tau^2}\frac{d\tau}{\tau} \quad (4)$$

where $H(\tau)$ is the distribution function of the structural elements with relaxation time τ, and G_o is the equilibrium modulus with a zero value for viscoelastic liquids. Eqs. (3) and (4) can be generalized with a Fredholm integral equation of the first-kind, which takes the form:

$$g(s) = \int_a^b K(s,t)f(t)dt, \quad \alpha \le s \le \beta \quad (5)$$

where $K(s,t)$ is the kernel that describes the system being $(\omega^2\tau^2/(1+\omega^2\tau^2)$ and $\omega\tau/(1+\omega^2\tau^2)$ for Eqs. (3) and (4), respectively, $g(s)$ is the measured signal ($G'(\omega)$ or $G''(\omega)$) and $f(t)$ is the relaxation spectrum $H(\tau)$. Numerical integration determines the spectral function $f(t)$ that represents the relaxation pattern of the material. Spectra calculation proceeds with discretization of the kernels of functions (3) or (4) using an algorithm that is published elsewhere (Kontogiorgos, 2010). The master curves in Fig. 4 were then analyzed with the *L*-curve criterion followed by the Tikhonov regularization.

Discretization of Eqs. (3) and (4) was performed between 10^{-4} and 10^2 s using a heuristic approach. Calculation of the optimum regularization parameter, λ, is a necessary step as it controls the interplay between the regularization error and the loss of resolution (Hansen, 1994). The optimum regularization parameter is located at the corner of the *L*-curves in Fig. 6 (top right inset). The *x*-axis of the curve (residual norm) corresponds to solutions where the calculation error controls the solution, with the *y*-axis (solution norm) reflecting solutions that are sensitive to experimental noise. We show semi-logarithmic plots of relaxation spectra produced using both kernels of Eqs. (3) and (4).

The two viscoelastic functions returned qualitatively similar monomodal spectra centered around 0.015 s for the sample at pH 7.0. Differences in the intensity of the spectra follow the magnitude of the modulus values in the master curve. This is in very good agreement with relaxation times of various polysaccharides that have been previously reported in the literature (Rincon, Munoz, Ramirez, Galan, & Alfaro, 2014; Rodriguez-Rivero, Hilliou, Martin del Valle, & Galan, 2014). Although pH does not seem to affect the overall relaxation behavior, acidic samples tend to resolve more relaxation elements in Fig. 6 (bottom right inset). According to the coupling model (Ngai, 2000), the extent of interactions between neighboring segments relates to the distribution of relaxation times, with strongly interacting macromolecules exhibiting a broad distribution in contrast to those with rather weak molecular interactions. Modeling indicates distinct molecular interactions due to conformational differences, with more resolved relaxation elements occurring as the isoelectric point is approached. It should be stressed, however, although qualitatively different, the spectra

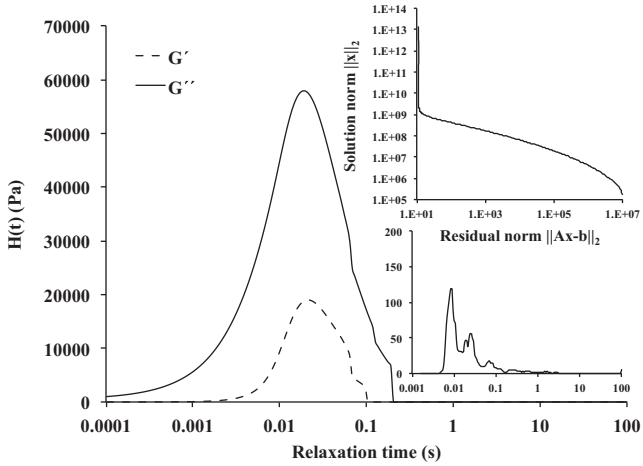

Fig. 6. Semi logarithmic plots of relaxation spectrum of 1% LM-pectin and 79% glucose syrup at pH 7.0 obtained using data from master curves in Fig. 4; Solid or dashed lines were obtained after discretization of the loss or storage modulus, respectively; Top right inset shows a typical shape of *L*-curves that were used to calculate the optimum regularization parameter, and bottom right inset shows the relaxation spectrum of 1% LM-pectin and 79% glucose syrup at pH 3.0.

reveal that that all relaxation processes are essentially complete within <~0.1 s regardless of pH.

This is an important observation that adds to the earlier discussion from the thermomechanical analysis for the identification of the molecular origin of interactions in the high-solid pectin system as a function of pH. This outcome indicates that discrepancies between the mechanical properties of the samples in the glass transition region stem from topological or steric restrictions in chain mobility in addition to the conformational changes that were induced with variations in the degree of ionization.

4. Conclusions

The influence of pH on the structural properties of non-gelling LM-pectin in the presence of co-solute has been investigated by means of thermomechanical analysis and theoretical modeling of results. Tuning pH at acidic or neutral conditions affects the conformation of the polysaccharide, hence impacting its micro- and macromolecular behavior within the experimentally accessible temperature range. Dissociation of galacturonic acid residues at the high pH values results in extended chain conformation and early vitrification events. Conversely, as the polyelectrolyte approaches its isoelectric point at low pH, recorded viscoelastic functions decrease and vitrification is delayed. Time–temperature superposition extended the experimental timeframe of observations yielding master curves of viscoelasticity and enabling calculation of the corresponding shift factors. These were utilized in WLF modeling to confirm the early vitrification of the pectin molecule in mixture with glucose syrup at neutral pH. Spectral analysis of the viscoelastic master curves revealed the exact positioning of the relaxation events characterized by one dominant regime where the relaxation of the macromolecules concludes.

References

Al-Ruqaie, I. M., Kasapis, S., Richardson, R. K., & Mitchell, G. (1997). The glass transition zone in high solids pectin and gellan preparations. *Polymer*, *38*(22), 5685–5694.

Alba, K., Laws, A. P., & Kontogiorgos, V. (2015). Isolation and characterisation of acetylated LM-pectins extracted from okra pods. *Food Hydrocoilloids*, (43), 726–735.

Alba, K., Ritzoulis, C., Georgiadis, N., & Kontogiorgos, V. (2013). Okra extracts as emulsifiers for acidic emulsions. *Food Research International*, *54*, 1730–1737.

Almrhag, O., George, P., Bannikova, A., Katopo, L., Chaudhary, D., & Kasapis, S. (2012). Analysis on the effectiveness of co-solute on the network integrity of high methoxy pectin. *Food Chemistry*, *135*(3), 1455–1462.

Behrouzian, F., Razavi, S. M. A., & Karazhiyan, H. (2014). Intrinsic viscosity of cress (*Lepidium sativum*) seed gum: Effect of salts and sugars. *Food Hydrocolloids*, *35*(0), 100–105.

Bohmer, R., Ngai, K. L., Angell, C. A., & Plazek, D. J. (1993). Nonexponential relaxations in strong and fragile glass formers. *The Journal of Chemical Physics*, *99*(5), 4201–4209.

Espitia, P. J. P., Du, W.-X., Avena-Bustillos, R. d. J., Soares, N. d. F. F., & McHugh, T. H. (2014). Edible films from pectin: Physical–mechanical and antimicrobial properties—A review. *Food Hydrocolloids*, *35*(0), 287–296.

Evageliou, V., Kasapis, S., & Hember, M. W. N. (1998). Vitrification of κ-carrageenan in the presence of high levels of glucose syrup. *Polymer*, *39*(17), 3909–3917.

Evageliou, V., Richardson, R. K., & Morris, E. R. (2000). Effect of pH, sugar type and thermal annealing on high-methoxy pectin gels. *Carbohydrate Polymers*, *42*(3), 245–259.

Fathi, M., Martin, A., & McClements, D. J. (2014). Nanoencapsulation of food ingredients using carbohydrate based delivery systems. *Trends in Food Science & Technology*, *39*(1), 18–39.

Ferry, J. D. (1980). *Viscoelastic properties of polymers*. New York, NY: Wiley.

Ghori, M. U., Alba, K., Smith, A. M., Conway, B. R., & Kontogiorgos, V. (2014). Okra extracts in pharmaceutical and food applications. *Food Hydrocolloids*, *42*, 342–347.

Grimm, A., Kruger, E., & Burchard, W. (1995). Solution properties of β-D-(1,3)(1,4)-glucan isolated from beer. *Carbohydrate Polymers*, *27*(3), 205–214.

Haines, P. J., Reading, M., & Wilburn, F. W. (2003). Differential thermal analysis and differential scanning calorimetry. In E. W. Brown (Ed.), *Handbook of thermal analysis and calorimetry*. Amsterdam: Elsevier.

Hansen, P.-C. (1994). Regularization tools: A MATLAB package for analysis and solution of discrete ill-posed problems. *Numerical Algorithms*, *6*, 1–35.

Jiang, B., Kasapis, S., & Kontogiorgos, V. (2011). Combined use of the free volume and coupling theories in the glass transition of polysaccharide/co-solute systems. *Carbohydrate Polymers*, *83*, 926–933.

Kasapis, S. (2008). Recent advances and future challenges in the explanation and exploitation of the network glass transition of high sugar/biopolymer mixtures. *Critical Reviews in Food Science and Nutrition*, *48*(2), 185–203.

Kasapis, S. (2012). Relation between the structure of matrices and their mechanical relaxation mechanisms during the glass transition of biomaterials: A review. *Food Hydrocolloids*, *26*(2), 464–472.

Kasapis, S., Al-Alawi, A., Guizani, N., Khan, A. J., & Mitchell, J. R. (2000). Viscoelastic properties of pectin–co-solute mixtures at iso-free-volume states. *Carbohydrate Research*, *329*(2), 399–407.

Kasapis, S., Al-Marhoobi, I. M., Deszczynski, M., Mitchell, J. R., & Abeysekera, R. (2003). Gelatin vs polysaccharide in mixture with sugar. *Biomacromolecules*, *4*(5), 1142–1149.

Kasapis, S., Al-Marhoobi, I. M., & Mitchell, J. R. (2003). Molecular weight effects on the glass transition of gelatin/cosolute mixtures. *Biopolymers*, *70*(2), 169–185.

Kasapis, S., Al-Marhoobi, I. M. A., & Khan, A. J. (2000). Viscous solutions, networks and the glass transition in high sugar galactomannan and κ-carrageenan mixtures. *International Journal of Biological Macromolecules*, *27*(1), 13–20.

Kim, Y., Williams, M. A. K., Galant, A. L., Luzio, G. A., Savary, B. J., Vasu, P., et al. (2013). Nanostructural modification of a model homogalacturonan with a novel pectin methylesterase: Effects of pH on nanostructure, enzyme mode of action and substrate functionality. *Food Hydrocolloids*, *33*(1), 132–141.

Kontogiorgos, V. (2010). Calculation of relaxation spectra from mechanical spectra in MATLAB. *Polymer Testing*, *29*, 1021–1025.

Mezger, G. T. (2011). *The rheology handbook*. Hanover: Vincentz Network.

Mohammad Amini, A., & Razavi, S. M. A. (2012). Dilute solution properties of Balangu (*Lallemantia royleana*) seed gum: Effect of temperature, salt, and sugar. *International Journal of Biological Macromolecules*, *51*(3), 235–243.

Ngai, K. L. (2000). Short-time and long-time relaxation dynamics of glass-forming substances: A coupling model perspective. *Journal of Physics: Condensed Matter*, *12*(29), 6437.

Panyoyai, N., Bannikova, A., Small, D. M., & Kasapis, S. (2015). Controlled release of thiamin in a glassy κ-carrageenan/glucose syrup matrix. *Carbohydrate Polymers*, *115*(0), 723–731.

Richardson, P. H., Willmer, J., & Foster, T. J. (1998). Dilute solution properties of guar and locust bean gum in sucrose solutions. *Food Hydrocolloids*, *12*(3), 339–348.

Rincon, F., Munoz, J., Ramirez, P., Galan, H., & Alfaro, M. C. (2014). Physicochemical and rheological characterization of *Prosopis juliflora* seed gum aqueous dispersions. *Food Hydrocolloids*, *35*(0), 348–357.

Rodriguez-Rivero, C., Hilliou, L., Martin del Valle, E. M., & Galan, M. A. (2014). Rheological characterization of commercial highly viscous alginate solutions in shear and extensional flows. *Rheologica Acta*, *53*(7), 559–570.

Roland, C. M. (2010). Relaxation phenomena in vitrifying polymers and molecular liquids. *Macromolecules*, *43*(19), 7875–7890.

Sengkhamparn, N., Bakx, E. J., Verhoef, R., Schols, H. A., Sajjaanantakul, T., & Voragen, A. G. J. (2009). Okra pectin contains an unusual substitution of its rhamnosyl residues with acetyl and alpha-linked galactosyl groups. *Carbohydrate Research*, *344*(14), 1842–1851.

Sengkhamparn, N., Verhoef, R., Schols, H. A., Sajjaanantakul, T., & Voragen, A. G. J. (2009). Characterisation of cell wall polysaccharides from okra (*Abelmoschus esculentus* (L.) Moench). *Carbohydrate Research*, *344*(14), 1824–1832.

Strom, A., Ribelles, P., Lundin, L., Norton, I., Morris, E. R., & Williams, M. A. K. (2007). Influence of pectin fine structure on the mechanical properties of calcium-pectin and acid-pectin gels. *Biomacromolecules*, *8*(9), 2668–2674.

Strom, A., Schuster, E., & Goh, S. M. (2014). Rheological characterization of acid pectin samples in the absence and presence of monovalent ions. *Carbohydrate Polymers*, *113*(0), 336–343.

Tschoegl, W. N. (1989). *The phenomenological theory of linear viscoelastic behavior*. Berlin: Springer-Verlag.

Vincken, J. P., Schols, H. A., Oomen, R., Beldman, G., Visser, R., & Voragen, A. G. J. (2003). Pectin—The hairy thing: Evidence that homogalacturonan is a side chain of rhamnogalacturonan I. In F. Voragen, H. Schols, & R. Visser (Eds.), *Advances in pectin and pectinase research* (pp. 91–105). Dordrecht: Kluwer Academic Publishers.

Wendlandt, M. (2005). *NLCSmoothReg*. http://www.mathworks.com/matlabcentral/fileexchange/7712-nlcsmoothreg

Williams, M. L., Landel, R. F., & Ferry, J. D. (1955). The temperature dependence of relaxation mechanisms in amorphous polymers and other glass-forming liquids. *Journal of the American Chemical Society*, *77*(14), 3701–3707.